

Room evacuation through two contiguous exits

I.M. Sticco^a, G.A. Frank^c, S. Cerrotta^a, C.O. Dorso^{a,b}

^a*Departamento de Física, Facultad de Ciencias Exactas y Naturales, Universidad de Buenos Aires, Pabellón I, Ciudad Universitaria, 1428 Buenos Aires, Argentina.*

^b*Instituto de Física de Buenos Aires, Pabellón I, Ciudad Universitaria, 1428 Buenos Aires, Argentina.*

^c*Unidad de Investigación y Desarrollo de las Ingenierías, Universidad Tecnológica Nacional, Facultad Regional Buenos Aires, Av. Medrano 951, 1179 Buenos Aires, Argentina.*

Abstract

Current regulations demand that at least two exits should be available for a safe evacuation during a panic situation. The second exit is expected to reduce the overall clogging, and consequently, improve the evacuation time. However, rooms having contiguous doors not always reduce the leaving time as expected. We investigated the relation between the door's separation and the evacuation performance. We found that there exists a separation distance range that does not really improve the evacuation time, or it can even worsen the process performance. To our knowledge, no attention has been given to this issue in the literature. This work reports how the pedestrian's dynamics differ when the separation distance between two exit doors changes and how this affects the overall performance.

Keywords:

Panic evacuation, Social force model, Clogging delay

PACS: 45.70.Vn, 89.65.Lm

1. Introduction

The practice of providing two doors for emergency evacuation can be traced back to the last Qing dynasty in China (1644-1911 AD). A mandatory regulation established that large buildings had to provide two fire exits [1]. This kind of regulations upgraded to current standard codes with detailed specifications on the exits position, widths and separations [2, 3].

8 Current regulations claim that the minimum door width should be 0.813 m
9 while the maximum door-leaf should not exceed 1.219 m [3, 4]. If more than
10 two doors are required, the distance between two of them must be at least
11 one-half or one-third of the room diagonal distance. But, no special require-
12 ments apply to the rest of the doors.

13
14 The rulings leave some space for placing the extra openings (*i.e.* those
15 above two exits) at an arbitrary separation distance. Thus, it is possible to
16 place a couple of doors on the same side of the room at any distance. The
17 special case of two contiguous doors has been examined throughout the lit-
18 erature [5, 6, 7, 8].

19
20 Kirchner and Schadschneider studied the pedestrians evacuation process
21 through two contiguous doors using a cellular automaton model [5]. The
22 agents were able to leave the room under increasing panic situations for be-
23 havioural patterns varying from individualistic pedestrians to strongly cou-
24 pled pedestrians moving like a *herd*. The evacuation time was found to be
25 independent of the separation distance between doors for the individualistic
26 pedestrians in a panic situation. But if the pedestrians were allowed to move
27 like a herd, an increasing evacuation time for small separation lengths (less
28 than 10 individuals size) was reported.

29
30 The above conclusions are not in complete agreement with the investi-
31 gation acknowledged in Ref. [6]. The authors assert that the total number
32 of pedestrians leaving the room per unit time slows-down for separation dis-
33 tances (between doors) smaller than four door widths [6]. This slow-down
34 is identified as a disruptive interference effect due to pedestrians crossing in
35 each other's path. For the particular case analyzed in this work, the threshold
36 of four door widths ($4d_w$) corresponds to the distance separation necessary
37 to distinguish two independent groups of pedestrians, each one surrounding
38 the nearest door.

39
40 Researchers called the attention on the fact that no matter how sepa-
41 rated the two contiguous doors are placed, the overall performance does not
42 improve twice with respect to a single exit (of the same total width). This
43 effect is attributed to some sort of pedestrian interference [6].

44
45 Although the above results were obtained for very narrow doors (*i.e.* sin-

gle individual width), further investigation showed that they also apply to doors allowing two simultaneous leaving pedestrians. However, this does not hold for a room with a single door [7]. In this case, it is true that the mean flux of evacuating people increases with an increasing door width, but the ratio flux per door width decreases [9].

It was observed in Ref. [5, 7] that the two contiguous doors should not be placed near the wall corners, since the side walls affect negatively the evacuation efficiency. No further explanation was given on this phenomenon, although the authors concluded this may cause a worsening in the evacuation performance for large separation distances between doors.

A recent investigation (Ref. [8]) on evacuation processes of cellular automata suggests that five distances should be taken into account when studying the evacuation performance: the total width of the openings (that is, adding the widths of each door), the doors separation distance, the width difference between the two doors, and the distance to the nearest corner.

From the results shown in Ref. [8], the evacuation time depends on the total width of the openings (if both doors have the same width). But, for a fixed total width of the opening, it appears that the optimal location of the exits depends on the doors separation distance.

Our investigation focuses on symmetric configurations with equally sized doors. At variance to the above mentioned literature, we examine the evacuation dynamics by means of the Social Force Model (SFM). An overview of this model can be found in Section 2.

In Section 3 we describe the specific settings for the evacuation processes. The measurement conditions for the simulations can also be found there.

In Sections 4.1 to 4.2.2 the single door configuration is revisited. Its purpose is to make easier the understanding of the two-doors configuration for very small separation distances d_g .

In Section 4.3 we examine the case of two separated doors. We explore the effect of increasing the separation distance d_g until the clogging areas close to each door become almost independent.

Section 5 resumes the pedestrians behavioural patterns, and its consequences on the evacuation performance, for the different door separation scenarios.

2. Background

2.1. The Social Force Model

The “social force model” (SFM) deals with the pedestrians behavioural pattern in a crowded environment. The basic model states that the pedestrians motion is controlled by three kind of forces: the “desire force”, the “social force” and the “granular force”. The three are very different in nature, but enter into an equation of motion as follows

$$m_i \frac{d\mathbf{v}^{(i)}}{dt}(t) = \mathbf{f}_d^{(i)}(t) + \sum_j \mathbf{f}_s^{(ij)}(t) + \sum_j \mathbf{f}_g^{(ij)}(t) \quad (1)$$

where m_i is the mass of the pedestrian i , and \mathbf{v}_i is its corresponding velocity. The subscript j represents all other pedestrians (excluding i) and the walls. \mathbf{f}_d , \mathbf{f}_s and \mathbf{f}_g are the desire force, the social force and the granular force, respectively. See Refs. [10, 9, 11, 12, 13] for details.

The desire force reflects the pedestrian’s own desire to go to a specific place [10]. He (she) needs to accelerate (decelerate) from his (her) current velocity, in order to achieve his (her) own willings. As he (she) reaches the velocity that makes him (her) feel comfortable, no further acceleration (deceleration) is required. This velocity is the “desired velocity” of the pedestrian $\mathbf{v}_d(t)$. The expression for \mathbf{f}_d in Eq. (2) handles this issue.

$$\begin{cases} \mathbf{f}_d^{(i)}(t) &= m_i \frac{\mathbf{v}_d^{(i)}(t) - \mathbf{v}_i(t)}{\tau} \\ \mathbf{f}_s^{(ij)} &= A_i e^{(r_{ij}-d_{ij})/B_i} \mathbf{n}_{ij} \\ \mathbf{f}_g^{(ij)} &= \kappa g(r_{ij} - d_{ij}) \Delta \mathbf{v}_{ij} \cdot \mathbf{t}_{ij} \end{cases} \quad (2)$$

109 τ means a relaxation time. Further details on each parameter can be
 110 found in Refs. [10, 9, 11, 12, 13].

111

112 Notice that the desired velocity \mathbf{v}_d has magnitude v_d and points to the
 113 desired place at the direction $\hat{\mathbf{e}}_d$. Thus, v_d represents his (her) state of anxi-
 114 ety, while $\hat{\mathbf{e}}_d$ indicates the place where he (she) is willing to go. We assume,
 115 for simplicity, that v_d remains constant during an evacuation process, but $\hat{\mathbf{e}}_d$
 116 changes according to the current position of the pedestrian.

117

118 The social force \mathbf{f}_s corresponds to the tendency of each individual to keep
 119 some space between him and other pedestrians, or, between him and the
 120 walls [14]. The \mathbf{f}_s expressed in Eq. (2) depends on the inter-pedestrian dis-
 121 tance d_{ij} . The magnitude $r_{ij} = r_i + r_j$ is the sum of the pedestrian's radius,
 122 while A_i and B_i are two fixed parameters ($r_j = 0$ for the interaction with the
 123 wall). Thus, \mathbf{f}_s is a repulsive monotonic force that resembles the pedestrian
 124 feelings for preserving his (her) *private sphere* [10, 14].

125

126 The granular force \mathbf{f}_g appearing in Eq. (1) represents the sliding friction
 127 between contacting people (or between people and walls). Its expression can
 128 be seen also in Eq. (2). It is assumed to be a linear function of the relative
 129 (tangential) velocities $\Delta\mathbf{v}_{ij} \cdot \mathbf{t}_{ij}$ of the contacting individuals. The function
 130 $g(r_{ij} - d_{ij})$ returns the argument value if $r_{ij} > d_{ij}$, while κ is a fixed param-
 131 eter (see Refs. [10, 9, 11, 12, 13]).

132

133 2.2. Clustering structures

134 The time delays during an evacuation process are related to clustering
 135 people as explained in Refs. [9, 11]. Groups of pedestrians can be defined as
 136 the set of individuals that for any member of the group (say, i) there exists
 137 at least another member belonging to the same group (j) in contact with the
 138 former. That is,

$$i \in \mathcal{G} \Leftrightarrow \exists j \in \mathcal{G} / d_{ij} < r_i + r_j \quad (3)$$

139 where \mathcal{G} corresponds to any set of individuals. This kind of structure is called
 140 a *human cluster*.

141

142 From all human clusters appearing during the evacuation process, those
 143 that are simultaneously in contact with the walls on both sides of the exit

are the ones that possibly *block* the way out. Thus, we are interested in the minimum number of contacting pedestrians belonging to this *blocking cluster* that are able to link both sides of the exit. We call this minimalistic group as a *blocking structure*. Any blocking structure is supposed to work as a barrier for the pedestrians in behind.

2.3. The local pressure on the pedestrians

The pressure on a single pedestrian (say, i) is defined as [10]

$$P_i = \frac{1}{2\pi r_i} \sum_{j=1}^{N-1} \mathbf{f}_s^{(ij)} \cdot \mathbf{n}_{ij} \quad (4)$$

$\mathbf{f}_s^{(ij)}$ are the forces acting on the individual i due to the other individuals. Recall that these forces point from any individual j to the individual i , and thus, the products $\mathbf{f}_s^{(ij)} \cdot \mathbf{n}_{ij}$ are always positive.

Notice that Eq. (4) holds either if the pedestrians are in contact or not. The feelings for preserving the *private sphere* actuate as a “social pressure” that makes possible for the individuals to change their behavioural pattern when they come too close to each other or to the walls.

A more formal definition for the “social pressure” is given in Appendix A. We show that the definition (4) is in accordance with the one in Appendix A, if the momentum p_i of the individuals become neglectable. Thus, the expression (4) is suitable for clogging situations where the pedestrians move slowly.

We further applied the formal definition for the “social pressure” to a simple example in Appendix B. We also checked that both definitions give the same results all through Section 4.

3. Numerical simulations

3.1. Geometry and process simulation

We simulated different evacuation processes for room sizes of 20 m × 20 m, 30 m × 30 m and 40 m × 40 m. The rooms had one or two exit doors

175 on the same wall, as shown in Fig. 1. The doors were placed symmetrically
176 from the mid position of the wall, in order to avoid corner effects. Both doors
177 had also the same width.

178
179 At the beginning of the process, the pedestrians were all equally sepa-
180 rated in a square arrangement. The occupancy density was initially set to
181 0.6 people/m², close to the allowed limiting values by current regulations [15].
182 They all had random velocities resembling a Gaussian distribution with null
183 mean value. The pedestrians were willing to go to the nearest exit. Thus, all
184 the pedestrians had the desired velocity \mathbf{v}_d pointing to the same exit door if
185 only one door was available, or to the nearest door if two exits were available.

186
187 In order to focus on the effects due to dual exits, we only allowed the
188 pedestrians to move individualistically, that is, neither leaderships nor herd-
189 ing behaviors were present during the evacuation process. At any time, the
190 pedestrians knew the doors location and tried to escape by their own.

191
192 The simulations were supported by LAMMPS molecular dynamics simula-
193 tor with parallel computing capabilities [16]. The time integration algorithm
194 followed the velocity Verlet scheme with a time step of 10^{-4} s. All the nec-
195 essary parameters were set to the same values as in previous works (see
196 Refs. [12, 13]). It was assumed that all the individuals had the same radius
197 ($r_i = 0.3$ m) and weight ($m_i = 70$ kg). We ran 30 processes for each panic
198 situation, in order to get enough data for mean values computation.

199
200 Although the LAMMPS simulator has the most common built-in functions,
201 neither the social force \mathbf{f}_s nor the desire force \mathbf{f}_d were available. We imple-
202 mented special modules (with parallel computing compatibilities) for the \mathbf{f}_s
203 and \mathbf{f}_d computations. These computations were checked over with previous
204 computations.

205
206 The pedestrian's desired direction $\hat{\mathbf{e}}_d$ was updated at each time step. Af-
207 ter leaving the room, they continued moving away. No re-entering mechanism
208 was allowed.

209

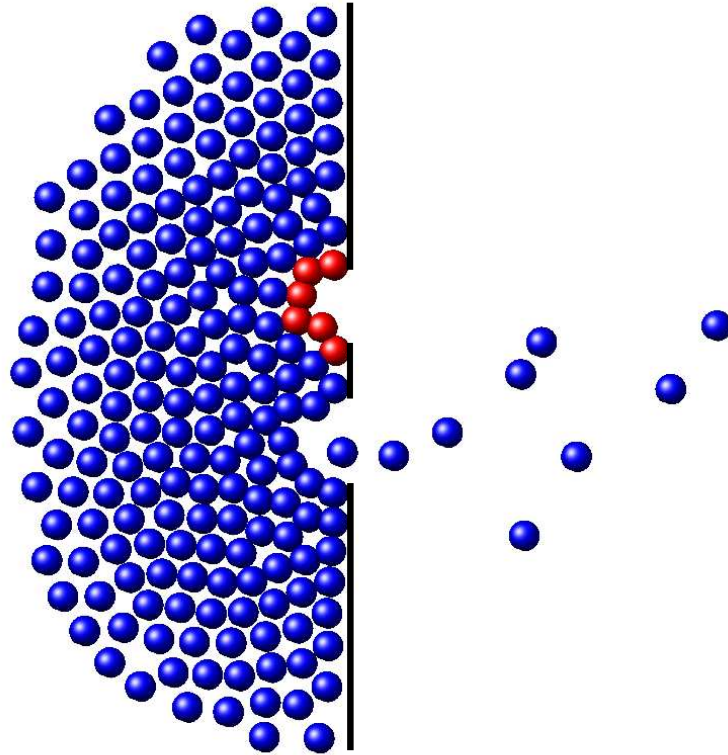


Figure 1: Snapshot of an evacuation process from a $20\text{ m} \times 20\text{ m}$ room, with two doors. In red we can see a blocking structure around the upper door. The desired velocity was $v_d = 4\text{ m/s}$.

210 3.2. Measurements conditions

211 Simulations were run in the same way as in Refs. [12, 13]. Each process
212 started with all the individuals inside the room. The measurement period
213 lasted until 80% of the occupants left the room. If this condition could not be
214 fulfilled within the first 3000 s, the process was stopped. Data was recorded
215 at time intervals of 0.05 s (cf. Eq. (2a)).

216
217 The simulations ran from relaxed situations ($v_d < 2$ m/s) to very stressing
218 rushes ($v_d = 8$ m/s). We registered the individuals positions and velocities
219 for each evacuation process. Thus, we were able to compute the “social
220 pressure” through out the process and to trace the pedestrians behavioural
221 pattern.

223 4. Results

224 4.1. The faster is slower effect

225 As a starting point, we checked over the “faster is slower” effect for the
226 room with two doors on the same wall. Fig. 2 shows the recorded evacuation
227 time when the doors are separated a distance of $d_g = 1$ m and when no sep-
228 aration exists at all ($d_g = 0$). The latter means a single opening with width
229 equal to two doors. Both cases (with or without separation) exhibit a change
230 in their corresponding slopes. Thus, the “faster is slower” effect is achieved
231 following the same qualitative response as the one found in previous works
232 for rooms with a single exit [10, 9].

233
234 The evacuation time for separated doors in Fig. 2 is always above the
235 time required to evacuate the pedestrians through the single opening (*i.e.*
236 null separation). For $v_d = 6$ m/s, the single opening improves the evacuation
237 performance in half of the time that demands the $d_g = 1$ m separation config-
238 uration. Other separation distances (not shown) exhibit the same qualitative
239 pattern as the example presented in Fig. 2. Therefore, it is clear that while
240 the total width of the opening remains unchanged, splitting this width into
241 to symmetric exits affects significantly the evacuation performance.

242
243 We made further research on the $d_g = 0$ and $d_g > 0$ scenarios. The former
244 is investigated in Section 4.2, while the latter is left to Section 4.3.

245

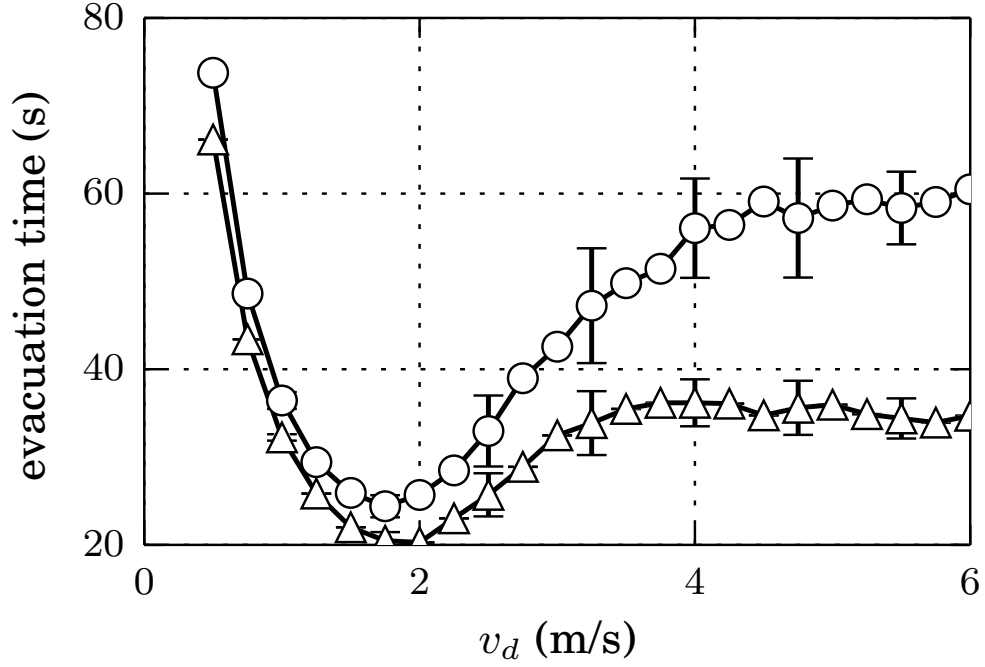


Figure 2: Mean evacuation time for 160 individuals (seconds) vs. the pedestrian's desired velocity (m/s). The room was 20×20 m size. Two contiguous doors were placed on one side of the room as shown in Fig. 1 (see text for details). Mean values were computed from 30 evacuation processes. Each door was $d_w = 1.2$ m width. The desired velocity was $v_d = 4$ m/s. Two situations are shown: Δ corresponds to the null separation distance between doors, meaning a single door of $2d_w$ width. \circ corresponds to the 1 m separation distance between doors ($d_g = 1$ m).

246 4.2. The single door vs. the null separation

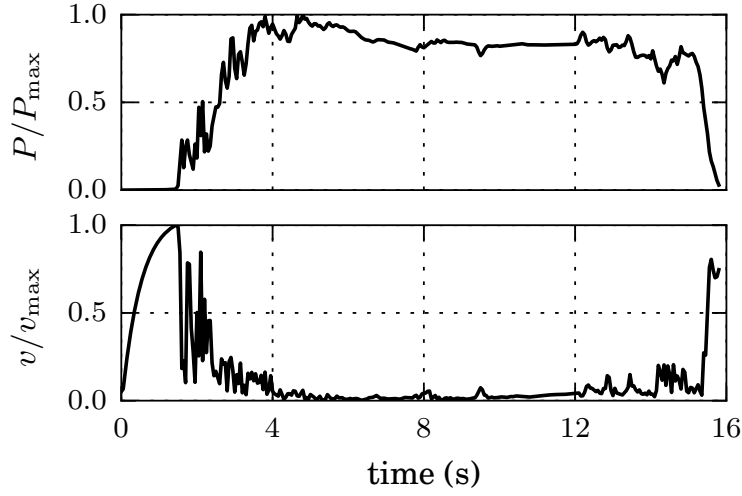
247 Recall that the $d_g = 0$ scenario corresponds to a single opening, but the
 248 total width of the opening is twice the width of a single door (see Section 4.1).
 249 Actually, it resembles the situation of a double sheet door.

251 4.2.1. The stop-and-go process

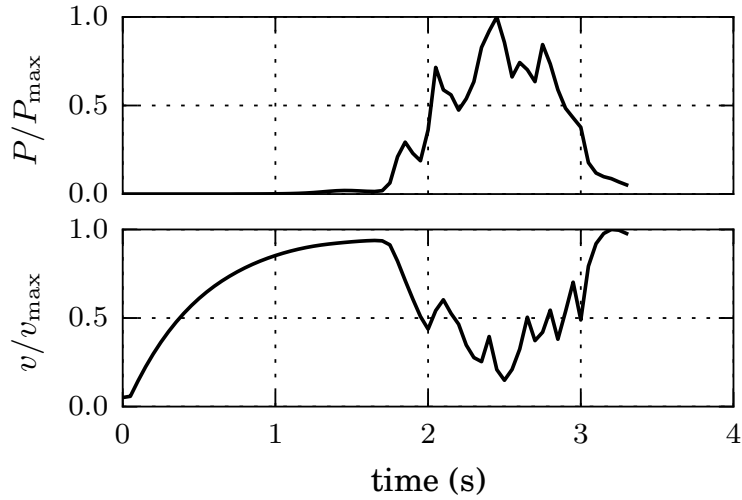
252 Fig. 3 illustrates on how the evacuation performance improves as the
 253 opening becomes wider. Fig. 3a corresponds to the single door ($d_w = 1.2$ m),
 254 while Fig. 3b corresponds to a wider opening ($3d_w = 3.6$ m), resembling
 255 a multi-leaf opening. Both figures represent the time evolution of a sin-
 256 gle pedestrian during an evacuation process. We can see the (normalized)
 257 pressure acting on the pedestrian and his (her) corresponding velocity. The
 258 starting point of the pedestrian was $(x, y) = (12.35$ m, 8.45 m). Notice that
 259 an increase in the opening width from d_w to $3d_w$ (Fig. 3a and Fig. 3b, re-
 260 spectively) reduces the evacuation time by one-fifth approximately.

261
 262 The pedestrian represented in Fig. 3 increases his (her) velocity towards
 263 an asymptotic value at the beginning of the processes. This value corre-
 264 sponds to the desired velocity $v_d = 4$ m/s. But close to $t = 2$ s, the pedes-
 265 trian suddenly stops because of the clogging around the exit. Clogging is also
 266 responsible for the pressure increase, as shown in both Fig. 3a and Fig. 3b.
 267 This can be checked over by means of Eq. (2) because when the velocity of
 268 the pedestrian vanishes, the desire force \mathbf{f}_d attains a maximum (in panic sit-
 269 uations only). Notice, however, that any further fluctuation of the pressure
 270 acting on the pedestrian corresponds to an inverse fluctuation on the velocity.
 271 Thus, the pedestrian is able to reach the exit following a stop-and-go process.

272
 273 The instantaneous pressure acting on a single pedestrian can be computed
 274 from Eq. (4) for a slow moving pedestrian (that is, $p_i \simeq 0$). The maximum
 275 pressure values P_{\max} in Fig. 3a and Fig. 3b are 8550 N.m $^{-1}$ and 6475 N.m $^{-1}$,
 276 respectively. The corresponding mean pressure values (after the first 2 s)
 277 are 80% and 55% of the respective maximum values. This means that the
 278 mean pressure value for the $3d_w$ situation is lower than the corresponding
 279 mean value for the d_w situation. That is, the wider opening seems to re-
 280 lease pressure from time to time. Consequently, the stop-and-go processes
 281 are somehow different for the single door with respect to the $d_g = 0$ situation



(a) Opening of $d_w = 1.2$ m width.



(b) Opening of $3d_w = 3.6$ m width.

Figure 3: Normalized pressure and velocity on a single pedestrian during an evacuation process. Data was recorded from the the initial position at $x = 12.35$ m and $y = 8.45$ m, until the individual left the room ($x > 20$ m). The pedestrians desired velocity was $v_d = 4$ m/s. Two situations are shown: (a) evacuation through a single door of width $d_w = 1.2$ m. (b) evacuation through an opening of $3d_w = 3.6$ m.

282 (the wider opening).

283

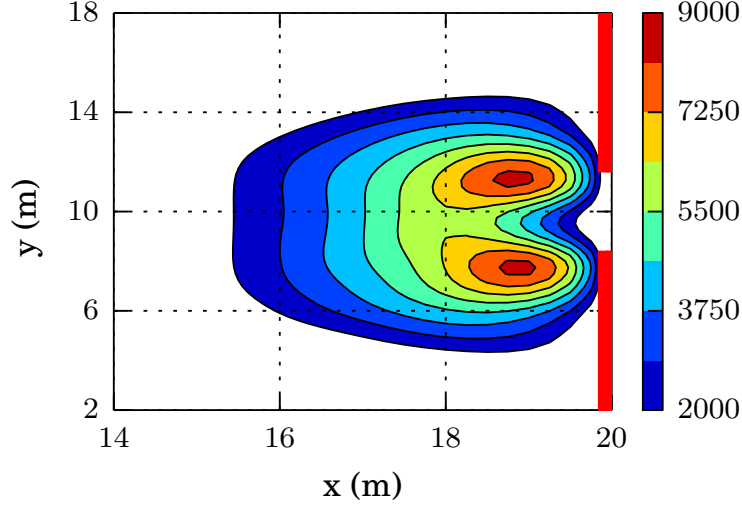
284 4.2.2. *The pressure and stream patterns*

285 For a better understanding on how the pedestrians are (intermittently)
286 released from high pressures in the wide opening situation, we pictured the
287 whole scene into a pressure contour map and a mean stream path map for all
288 the individuals. Fig. 6c shows the pressure levels (P_i) for the clogging area.
289 The warm colors are associated to high pressure values. These values are
290 close to the corresponding maximum pressure values (not shown). Thus, the
291 warm regions define the places where the pedestrians slow down most of the
292 time. They are expected to get released only for short periods of time. On
293 the contrary, the regions represented in cold colors (low mean pressure) are
294 those where the individuals are able to get released for longer time periods.

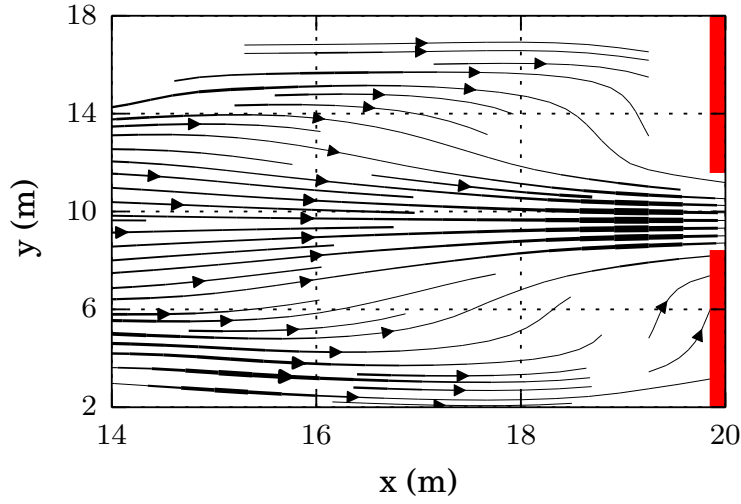
295

296 Fig. 4b represents the mean stream lines during the evacuation process.
297 It completes the stop-and-go picture since it exhibits the released paths for
298 leaving the room. Notice that the stream lines pass through the low pressure
299 regions. That is, it can be seen in Fig. 4b that the stream lines gather along
300 the middle of the clogging area, where “cold” pressure colors can be found
301 (cf. Fig. 6c). The “warm” pressure colors are placed on the sides of this
302 region.

303

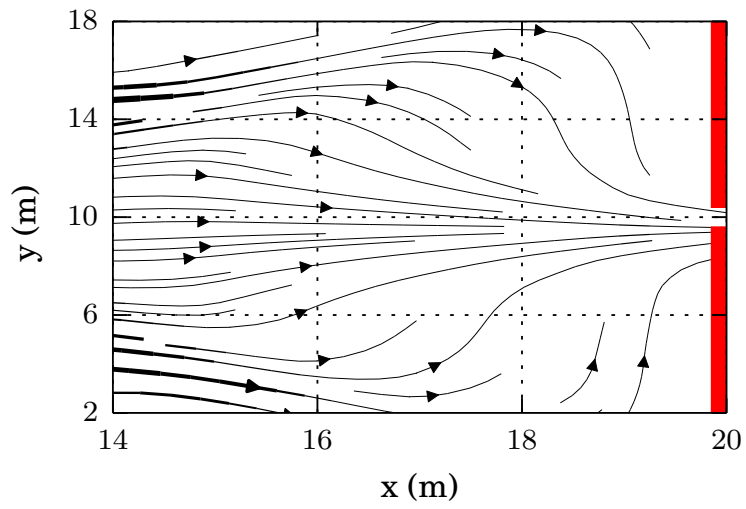


(a) Mean pressure contour lines (N.m^{-1} units). Colors in the on-line version only.



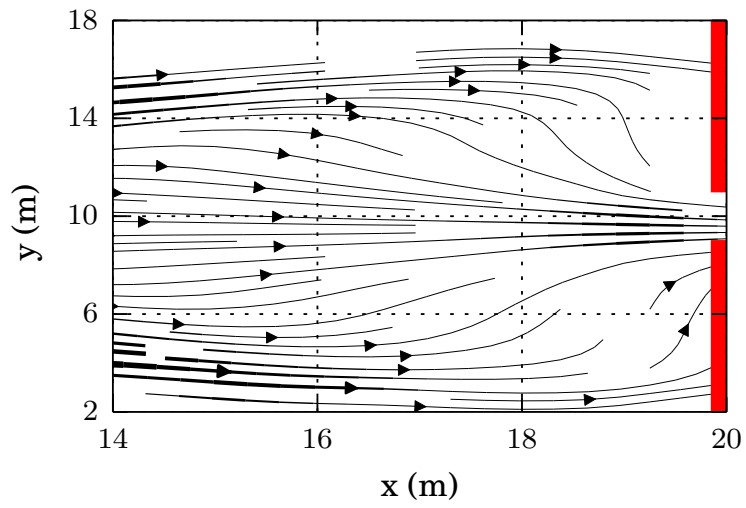
(b) Mean stream lines. The lines connect the normalized velocity field (v/v_{\max}). The arrows indicate the stream direction.

Figure 4: Mean pressure and stream lines computed from 30 evacuation processes until 100 pedestrians left the room ($20\text{ m} \times 20\text{ m}$ size). Data was recorded on a square grid of $1\text{ m} \times 1\text{ m}$ and then splined to get smooth curves. The red lines at $x = 20\text{ m}$ represent the walls on the right of the room. There is only one opening of $3d_w = 3.6\text{ m}$ width (null separation distance between doors of width $3d_w/2$). The pedestrian's desired velocity was $v_d = 4\text{ m/s}$.



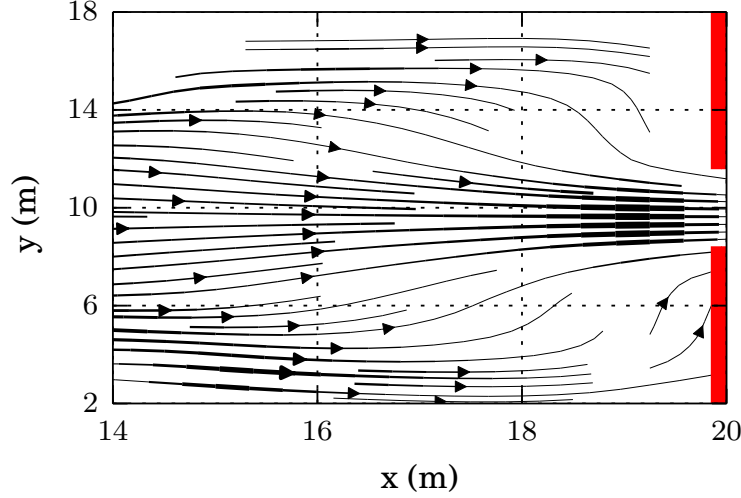
304

(a) Opening of $d_w = 1.2$ m width.



305

(b) Opening of $2d_w = 2.4$ m width.



(c) Opening of $3d_w = 3.6$ m width.

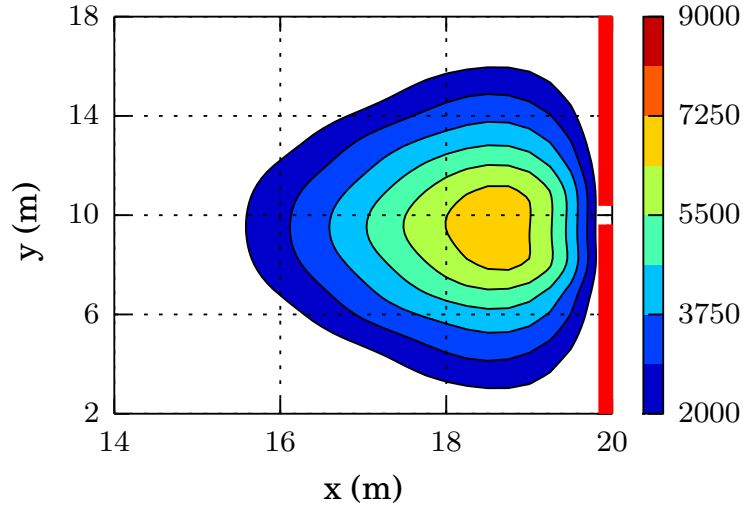
Figure 5: Mean stream lines computed from 30 evacuation processes until 100 pedestrians left the room ($20\text{ m} \times 20\text{ m}$ size). The lines connect the normalized velocity field (v/v_{\max}). The arrows indicate the stream direction. Data was recorded on a square grid of $1\text{ m} \times 1\text{ m}$ and then splined to get smooth curves. The red lines at $x = 20\text{ m}$ represent the walls on the right of the room. The pedestrian's desired velocity was $v_d = 4\text{ m/s}$ for all the cases.

We checked over the trajectory of the single pedestrian represented in Fig. 3b and we observed that he (she) managed to get out of the room through the path where the stream lines get denser. Thus, Fig. 3b resembles the stop-and-go process for the pedestrians passing through the middle of the clogging area, that is, along the low pressure (middle) region. The pedestrians on the sides of this region (high pressure region) are expected to slow down since Fig. 4b shows no stream lines to the exit.

Recalling the results in Fig. 3a for the same single individual as in Fig. 3b, we realize that the single door scene is likely to differ from the $d_g = 0$ situation since both patterns (for the same individual) do. Thus, we examined the pressure contour map for the single door and for an opening of twice the single door width. The results are shown in Fig. ???. Fig. 6b exhibits a similar pressure map pattern as Fig. 6c, but the single door pressure map in Fig. 6a does not. For the single door situation, we do not observe the lower pressure pathway in the middle of the clogging area. Instead, high pressure

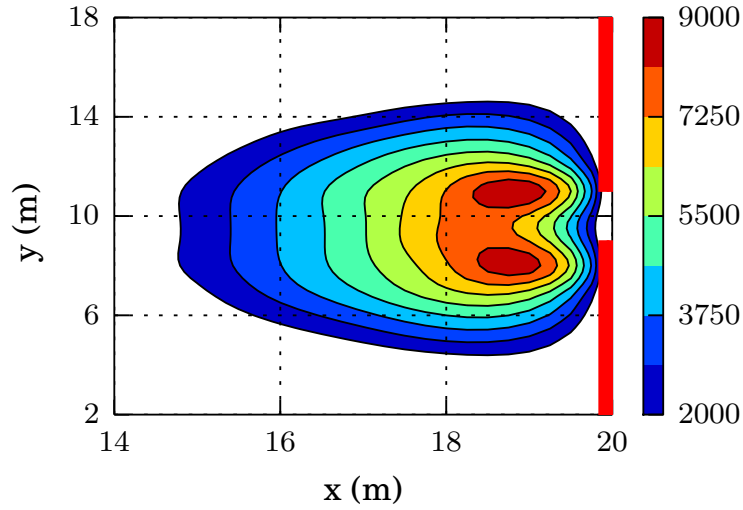
324 is acting on the pedestrians, as shown in the (normalized) pressure evolution
 325 in Fig. 3a. The corresponding velocity evolution (Fig. 3a) informs that the
 326 pedestrians in this region experience a slow down.

327



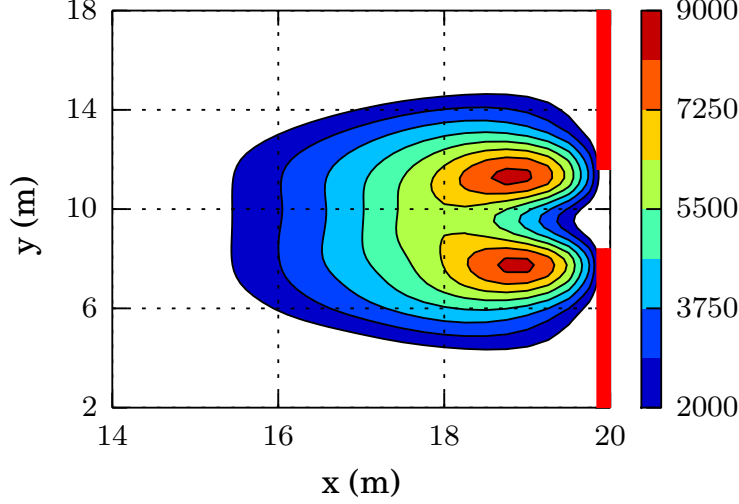
328

(a) Opening of $d_w = 1.2$ m width.



329

(b) Opening of $2d_w = 2.4$ m width.



(c) Opening of $3d_w = 3.6$ m width.

Figure 6: Mean pressure contour lines computed from 30 evacuation processes until 100 pedestrians left the room ($20\text{ m} \times 20\text{ m}$ size). The scale bar on the right is expressed in N.m^{-1} units (see text for details). The red lines at $x = 20\text{ m}$ represent the walls on the right of the room. The pedestrian's desired velocity was $v_d = 4\text{ m/s}$. The contour lines were computed on a square grid of $1\text{ m} \times 1\text{ m}$ and then splined to get smooth curves. Level colors can be seen in the on-line version only.

At this stage of the investigation we are able to point out a few conclusions. The widening of the single door increases the pedestrian's flux, as asserted in Ref. [7]. In the narrow situation (see Fig. 3a), the pedestrians experience a slow down. The corresponding time delays have been associated to blocking structures (see Refs. [9, 11]) and causes the pressure acting on the nearby individuals to rise. Fig. 6a resembles this situation. However, as the opening widens (*i.e.* the null separation situation), the pressure pattern changes qualitatively (see Fig. 6c and Fig. 6b), allowing the pedestrians in the middle of the clogging area to make a pathway to the exit. This pathway corresponds to the breaking of the blocking structures.

4.3. Separated doors

We will now analyze the case in which the evacuation process is through two doors, symmetrically placed on the same side of the room. We will explore the dependence of such a process on the doors separations. We will

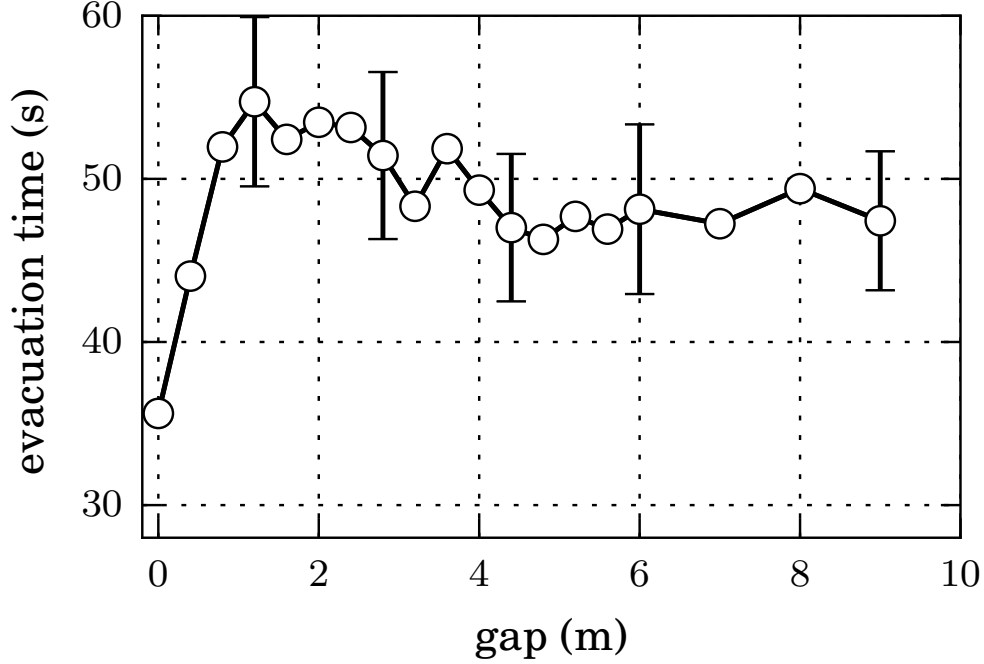


Figure 7: Mean evacuation time for 225 pedestrians (room of 20×20 m size) as a function of the doors separation distance. Mean values were computed from 30 evacuation processes until 160 pedestrians left the room. Each door was $d_w = 1.2$ m width for non-vanishing gaps. The null gap means a single door of $2d_w$ width. The desired velocity was $v_d = 4$ m/s.

347 assume that each door width is $d_w = 1.2$ m.

348

349 It has been shown in Fig. 2 that separating the doors a distance $d_g = 1$ m
 350 worsens the evacuation performance with respect to the null separation. We
 351 further explored this worsening by increasing d_g at steps of 0.5 m, starting
 352 from the null separation distance. Fig. 7 shows the mean evacuation time
 353 and the corresponding error bars (indicating the $\pm\sigma$ limits). The desired
 354 velocity was set to $v_d = 4$ m/s, where the “faster is slower” effect takes place.

355

356 The evacuation time as a function of d_g shown in Fig. 7 is one of our main
 357 results. The worsening in the evacuation performance rises to a maximum
 358 value at 1 m while its slope changes sign for $d_g > 1$ m. Thus, $d_g = 1$ m ap-
 359 pears to be the worst evacuation scenario for the $20 \text{ m} \times 20 \text{ m}$ room with 225

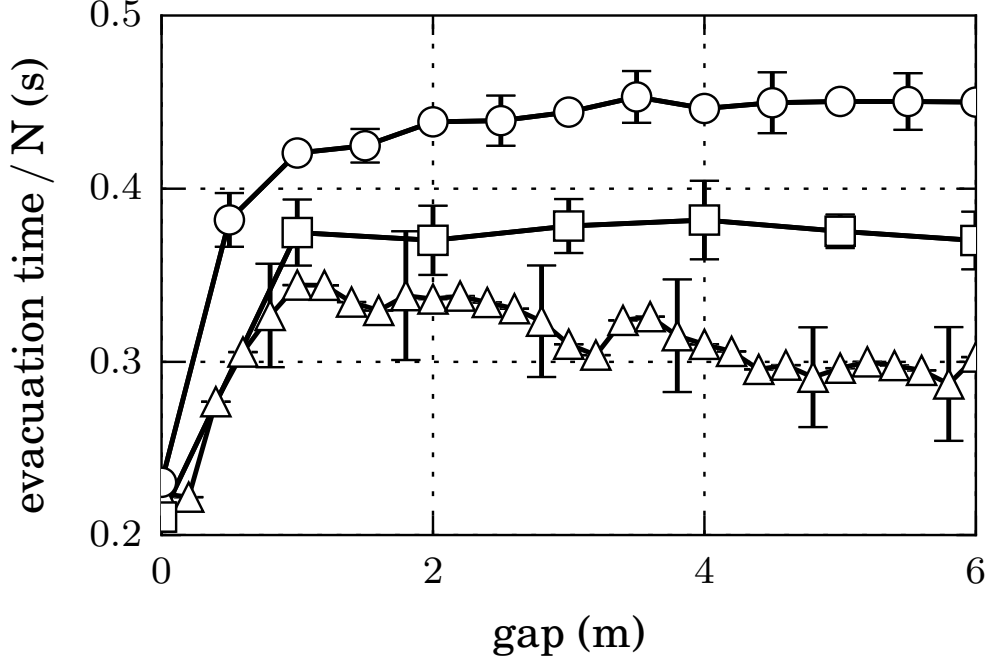


Figure 8: Mean evacuation time per total number of pedestrians that left the room (N), as a function of the doors separation distance. Mean values were computed from 30 evacuation processes. Each door was $d_w = 1.2$ m width for non-vanishing gaps. The null gap means a single door of $2d_w$ width. Three situations are shown: \triangle corresponds to the 20×20 m room when 160 pedestrians left the room, \square corresponds to 30×30 m room when 530 pedestrians left the room, and \circ corresponds to 40×40 m room when 865 pedestrians left the room. The desired velocity was $v_d = 4$ m/s.

360 individuals and two doors of $d_w = 1.2$ m each (see Fig. 7).

361

362 We further computed the mean evacuation time for an increasing number
 363 of pedestrians (and room sizes). We kept the pedestrian density unchanged
 364 (at $t = 0$) for all the simulation processes. Fig. 8 exhibits the mean evacua-
 365 tion time per pedestrian as a function of the separation distance (*i.e.* gap).
 366 We divided the evacuation time by the total number of pedestrians for visu-
 367 alization reasons.

368

369 The results shown in Fig. 8 were not expected. The evacuation time set-
 370 tles to an asymptotic value for separation distances $d_g > 5$ m. The mean

371 evacuation time becomes almost independent of the separation distances d_g
 372 despite that the clogging areas around the doors might still overlap.

373

374 Fig. 8 also shows that the slope not always changes sign at $d_g \simeq 1$ m.
 375 Furthermore, as the number of pedestrians is increased for $d_g > 1$ m, the
 376 evacuation time slope raises to positive values. The greater the number of
 377 pedestrians, the worst the evacuation time (per individual). This appears
 378 to occur for $d_g > 1$ m, regardless of the crowd size. That is, according to
 379 Fig. 8, there exists a separation distance value $d_g \simeq 1$ m where the evacua-
 380 tion slope changes sharply to negative or positive values (for $d_g > 1$ m). This
 381 phenomenon has not been studied in the literature, to our knowledge.

382

383 We can resume the results in Fig. 8 in the following way: the evacuation
 384 time rises when the doors separation increases from a wide opening (null
 385 separation distance) to the distance $d_g \simeq 1$ m. At this gap, the evacuation
 386 time slope changes notably, entering a much slowly varying regime towards
 387 an asymptotic value (for $d_g \gg 1$ m). The former can be identified as a regime
 388 for small values of d_g , while the latter is valid for moderate to large values
 389 of d_g . The fact that a sharp change occurs at $d_g \simeq 1$ m, no matter the crowd
 390 size, suggests that both regimes are somehow different in nature. This moved
 391 us to explore the two regimes separately.

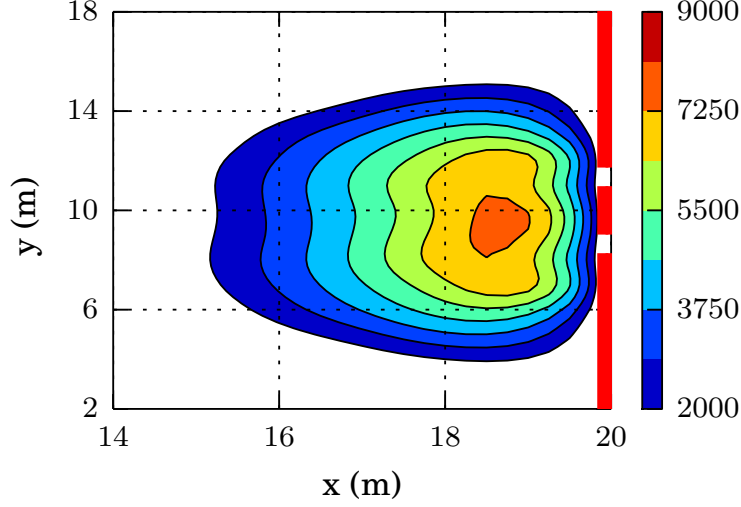
392

393 4.3.1. *The regime for $d_g < 1$ m*

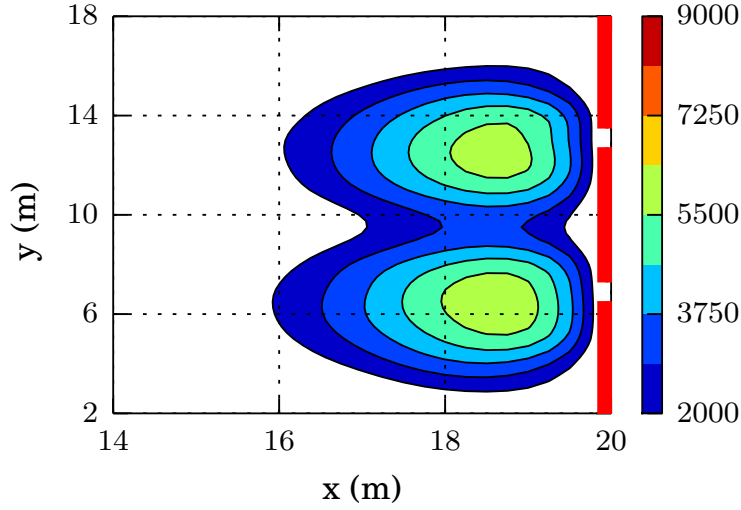
394 Our starting point is the pressure contour map, since we can easily com-
 395 pare the current patterns with those presented in Section 4.2.2. Fig. 9a shows
 396 the mean pressure pattern for the separation distance $d_g = 1.5$ m, that is,
 397 close to the gap value where the sharp change in the slope occurs. The dif-
 398 ferences between Fig. 9a and Fig. ?? are noticeable. We can now see a wide
 399 region in the center of the clogging area representing the high pressure (P_i)
 400 acting on each pedestrian (warm colors in Fig. 9a). The regularity in the col-
 401 ors of this region is meaningful: the high pressure acting on the pedestrians
 402 does not allow a regular stream (pathway) to the exit. This is in agreement
 403 with the evacuation time worsening shown in Fig. 7.

404

405 Fig. 9a suggests that blocking structures might be present for long time
 406 periods, since the pedestrians cannot manage to get out easily. We examined
 407 this possibility through the *blocking probability*. In this context, the block-



(a) Separation distance of $d_g = 1.5$ m.



(b) Separation distance of $d_g = 5$ m.

Figure 9: Mean pressure contour lines computed from 30 evacuation processes until 100 pedestrians left the room ($20\text{ m} \times 20\text{ m}$ size). The scale bar on the right is expressed in N.m^{-1} units (see text for details). The red lines at $x = 20\text{ m}$ represent the walls on the right of the room. The pedestrian's desired velocity was $v_d = 4\text{ m/s}$. The contour lines were computed on a square grid of $1\text{ m} \times 1\text{ m}$ and then splined to get smooth curves. Level colors can be seen in the on-line version only.

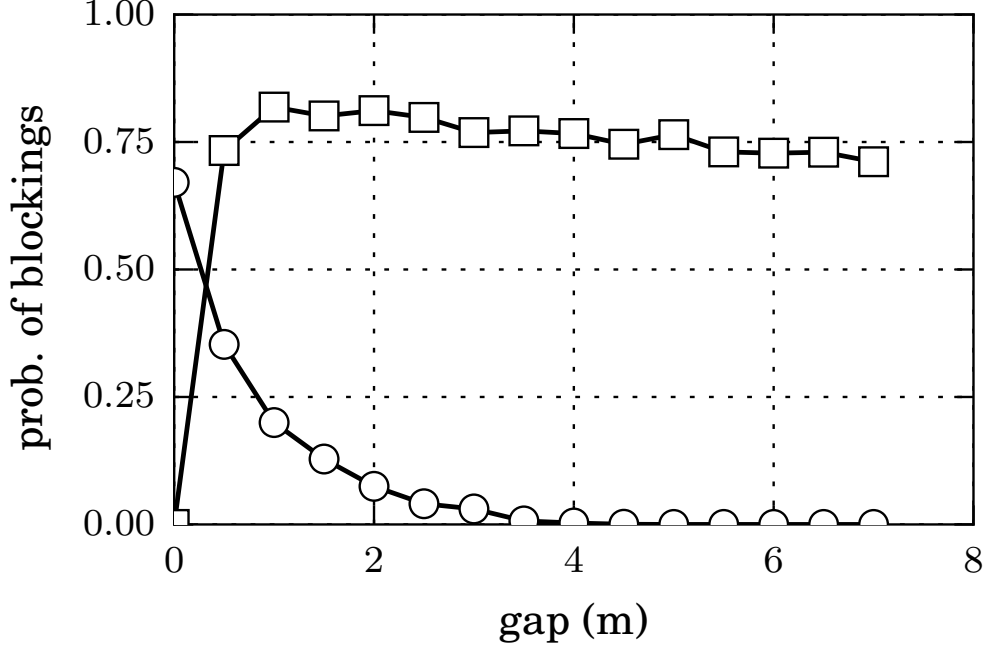


Figure 10: Ratio between time steps including blocking structures and the total number of time steps for 30 evacuation processes, as a function of the doors separation distance. The room size was 20×20 m with 225 occupants. Each door was $d_w = 1.2$ m width for non-vanishing gaps. The null gap means a single door of $2d_w$ width. The desired velocity was $v_d = 4$ m/s. ○ corresponds blocking structures connecting both the left side wall of the left door with the right side wall of the right door (see text for details). □ corresponds to blocking structures connecting both sides of a single door (see text for details).

ing probability is associated to the ratio between the time that each door
remains blocked with respect to the total evacuation time (cf. Section 2.2).
Fig. 10 presents two kinds of blockings: the simultaneous blocking of both
doors, and the blocking of a single door (say, the one on the left). The former
connects the left most wall with the right most wall, but does not contact
the separation wall in the middle of the walls. The latter connects the walls
on both sides of the selected door (say, the one on the left).

According to Fig. 10, the single door blockings are not relevant until
 $d_g \simeq 1$ m, while the simultaneous blockings weaken as the gap (separation
distance d_g) increases. The single door blockings resemble the response in

Fig. 7, and thus, we conclude that this kind of blockings should play an important role in the increase of the evacuation time for small gaps d_g . Notice that single door blocking probability explains the 75% of the evacuation time, as can be seen in Fig. 10.

The results so far moved us to focus closer on the dynamics around each door. We watched many animations of the evacuation process for gap distances between the null separation to $d_g = 1.5$ m (not shown). We realized that single door blockings hold if the gap is large enough to accommodate at least two pedestrians. That is, any blocking structure enclosing a single door can hold for some time if the pedestrians at the end of the structure (and in contact with the walls) do hardly leave the structure. Two pedestrians are needed at the gap wall to ensure that both doors remain blocked.

We want to call the attention on the fact that when d_g passes through the 1 m situation, the kind of simultaneous blocking without contacting the gap wall, is replaced by the kind of single door blockings acting (usually) simultaneously. This achieves a qualitative different pressure and stream pattern. As shown in Fig. 6b, the widening of the exit allows a pathway through the middle of the clogging area. This is likely to occur even for very small gaps (see Fig. 10). However, the single door blockings follow a pressure pattern similar to Fig. 6a on each door. What we see in Fig. 9a is the combined pattern built from two single door patterns as in Fig. 6a.

We conclude from the analysis of small gaps ($d_g < 1$ m) that a door separation distance roughly equal to two pedestrian widths is critical. This distance allows persistent single door blockings. Small distances (close to the null separation) do not actually allow single door blockings to hold for long time. Thus, the role of $d_g = 2r_{ij}$ (two pedestrian's width) is decisive to move the evacuation process from one regime to another.

4.3.2. *The regime for $d_g > 1$ m*

Fig. 10 shows that the single door blockings (see Section 4.3.1) remains around 75% of the total evacuation time for $d_g > 1$ m (225 individuals in the room). We also computed this magnitude for situations with increasing number of individuals (see Fig. 11). The probability of single door blockings approaches unity as the crowd size increases. This means, according to

our definition of blocking probability, that the blocking time raises as the number of individuals increases. The gap distance, however, does not play a significant role for $d_g > 1$ m.

There is a noticeable difference between the evacuation time shown in Fig. 8 and the blocking probability exhibited in Fig. 11. Fig. 8 presents the evacuation time for three different room sizes and increasing number of pedestrians. The slope of the evacuation curve is negative for the 20×20 m room, it vanishes for the 30×30 m situation and it becomes slightly positive for the 40×40 m room (for $d_g > 1$ m). Thus, as the number of pedestrians increases, the slope of the evacuation time changes sign. However, this does not occur for the blocking probability (see Fig. 11). The slope of the blocking probability remains always negative for an increasing number of pedestrians (and desire velocities). Therefore, the changes in the slope observed in Fig. 8 cannot be explained by changes in the blocking time (*i.e.* blocking probability).

We checked the pressure patterns for $d_g > 4d_w$ (see Fig. 9b as an example). We came to the conclusion that since the evacuation slope in Fig. 8 changes with an increasing number of individuals, the whole bulk should be involved in this phenomenon. Therefore, we focused our investigation on the pressure contribution of the whole bulk.

As shown in Eq. (A.3) of Appendix A, we can realize that the pressure of the whole bulk (left-hand side) is related to the total desire force contribution (right-hand side). Thus, the pressure of the bulk can vary in two possible ways: if the desire force of the individuals (*i.e.* anxiety levels) changes, or, if the crowd size changes. An increase on either the number of evacuating pedestrians (N) or their corresponding anxiety level (v_d), will increase the pressure of the whole bulk. A simple example is presented in the Appendix.

Fig. 8 exhibits the evacuation time for an increasing number of pedestrians. But, an increase in the pedestrians anxiety level should resemble similar results, if the above reasonings are true. Fig. 12 shows the evacuation time as a function of the separation distance for two different desired velocities. As expected, the sharp change in the slope occurs around $d_g = 2r_{ij}$. Also the slope changes as the desired velocity (v_d) is increased (*i.e.* higher anxiety level). This confirms that the social pressure is responsible the slope

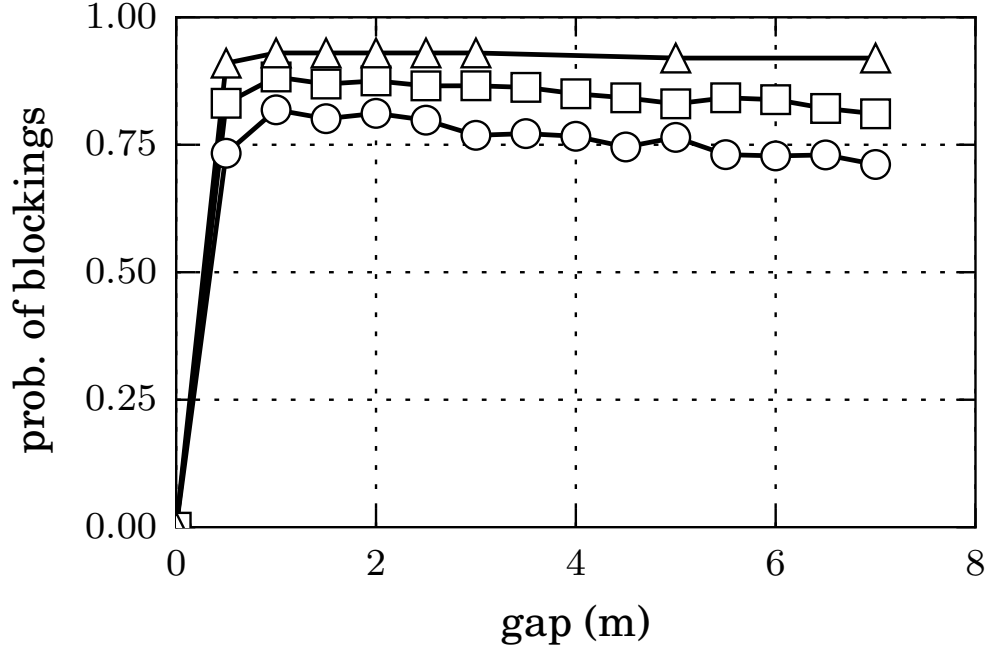


Figure 11: Ratio between time steps including blocking structures and the total number of time steps for 30 evacuation processes, as a function of the doors separation distance. The only blocking structures considered were those connecting both sides of one single door (see text for details). Each door was $d_w = 1.2$ m width for non-vanishing gaps. The null gap means a single door of $2d_w$ width. Three scenarios are shown: ○ corresponds to the room of size 20×20 m with 225 occupants and a desired velocity of $v_d = 4$ m/s. □ corresponds to the room of size 20×20 m with 225 occupants and a desired velocity of $v_d = 6$ m/s. △ corresponds to the room of size 40×40 m with 961 occupants and a desired velocity of $v_d = 4$ m/s.

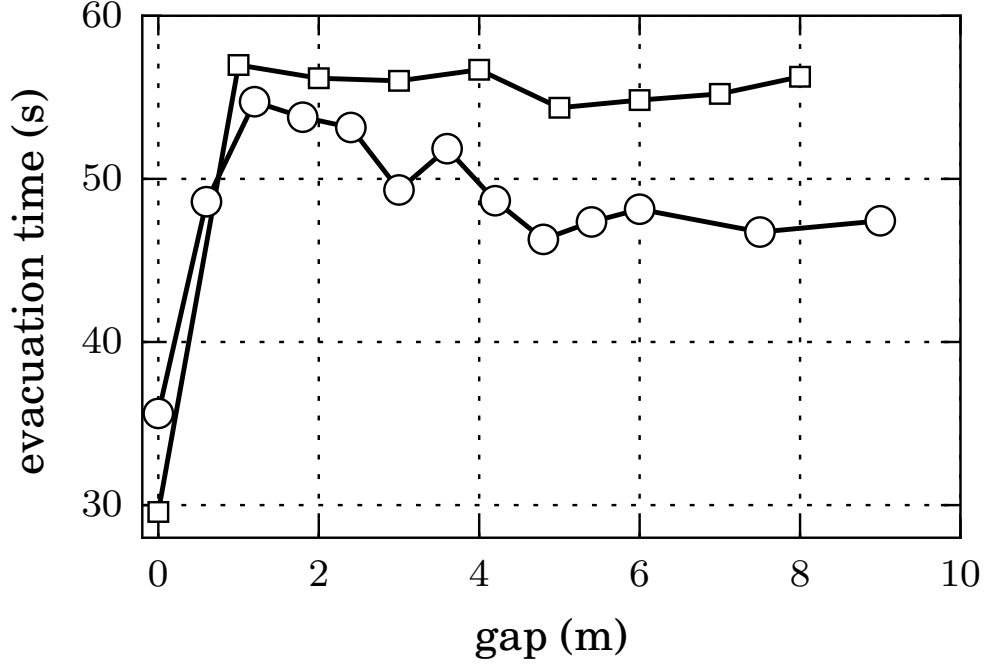


Figure 12: Mean evacuation time for 225 pedestrians (room of 20×20 m size) as a function of the doors separation distance. Mean values were computed from 30 evacuation processes until 160 pedestrians left the room. Each door was $d_w = 1.2$ m width for non-vanishing gaps. The null gap means a single door of $2d_w$ width. ○ corresponds to pedestrians with desired velocity of $v_d = 4$ m/s. □ corresponds to pedestrians with desired velocity of $v_d = 8$ m/s.

behaviour shown in Fig. 8.

We conclude from the analysis of large gaps ($d_g > 1$ m) that the evacuation time is controlled by the social pressure in the bulk. The crowd size and the desired velocity v_d affects the pressure acting on the pedestrians. For $d_g > 5$ m in our simulations, the evacuation time is very close to the corresponding asymptotic value, although the bulks around each door are not completely independent. This means that the mixing of both crowds (that is, the fact that the bulks are in contact) do not affect strongly the evacuation performance.

505 5. Conclusions

506 We examined in detail the evacuation of pedestrians for the situation
 507 where two contiguous doors are available for leaving the room. Throughout
 508 Section 4 we presented results on the evacuation performance under high
 509 anxiety levels and increasing number of pedestrians. Both conditions exhibit
 510 the novel result that a worsening in the evacuation time exists as the door
 511 separation distance d_g increases from the null value to roughly the width of
 512 two pedestrians. Special situations may enhance the evacuation performance
 513 for larger values of d_g .

514
 515 The range from $d_g = 0$ to $d_g \gg d_w$ was inspected. In the interval
 516 $0 \leq d_g \leq 2r_{ij}$ (two pedestrian's width), the evacuation performance worsened
 517 for all the explored situations, as the separation distance between doors d_g
 518 increased. But, from $d_g > 2r_{ij}$ the evacuation time enhanced for relatively
 519 small crowds and moderate anxiety levels. We realized that the sharp change
 520 in the evacuation behaviour at $d_g = 2r_{ij}$ corresponded to qualitative differ-
 521 ences in the pedestrian dynamics close to the exits.

522
 523 After a detailed comparison of the dynamics for the single door situation
 524 and for two doors very close to each other (that is, $d_g < 2r_{ij}$), we concluded
 525 that the blocking structures (*i.e.* blocking arcs) around the openings were
 526 released intermittently, allowing the pedestrians to leave the room in a stop-
 527 and-go process. As the separation distance approached $2r_{ij}$, the blocking
 528 arcs around each door, resembled the blocking situation of two single doors.
 529 This changes only affected the local dynamics (close to the doors), while the
 530 crowd remained gathered into a single clogging area.

531
 532 For $d_g > 2r_{ij}$ the single door blocking structures become relevant even
 533 for large values of d_g (see Fig. 10). No further qualitative changes were ob-
 534 served locally around each door. However, increasing the crowd size (N) or
 535 the pedestrian's anxiety level (v_d) slowed down the evacuation. Both mag-
 536 nitudes are linked to the pressure acting on the pedestrians, and therefore,
 537 enhanced the “faster is slower” effects.

538
 539 For a better understanding of the relationship between N , v_d and the
 540 pressure in the bulk, a simple lane example complemented our analysis. It
 541 was shown that the classical virial expression is still suitable for the investi-

542 gation of social systems.

543

544 6. Acknowledgments

545 C.O. Dorso is a main researcher of the National Scientific and Technical
546 Research Council (spanish: Consejo Nacional de Investigaciones Científicas
547 y Técnicas - CONICET), Argentina. G.A. Frank is an assistant researcher
548 of the CONICET, Argentina. I.M. Sticco and S. Cerrotta have degree in
549 Physics.

550 Appendix A. Alternative definition for the social pressure

551 Recall that the social force model (SFM) deals with the pedestrians de-
552 sire and their private space preservation. Although the desire force \mathbf{f}_d is a
553 “unilateral” force, the Newton equations of motion remain valid. Therefore,
554 it can be derived from the virial relation that [17]

$$\left\langle \sum_{i=1}^N \frac{p_i^2}{m_i} + \sum_{i=1}^N \mathbf{r}_i \cdot \mathbf{f}_i \right\rangle = -2\mathcal{P}\mathcal{A} \quad (\text{A.1})$$

555 for the set of N pedestrians inside an area \mathcal{A} . p_i and \mathbf{f}_i are the momentum
556 and total force acting on the individual i (excluding the interaction with the
557 walls). $\langle \cdot \rangle$ corresponds to the mean value along time. The right hand side
558 $-2\mathcal{P}\mathcal{A}$ defines the global pressure on the curve enclosing the surface \mathcal{A} .

559

560 Following Ref. [17] we can define the “social pressure function” P_i as

561

$$2P_i\mathcal{A}_i = \frac{p_i^2}{m_i} + \frac{1}{2} \sum_{j=1}^{N-1} \mathbf{r}_{ij} \cdot \mathbf{f}_s^{(ij)} \quad (\text{A.2})$$

562 where \mathcal{A}_i is the area enclosing the pedestrian i and $\mathbf{r}_{ij} = \mathbf{r}_i - \mathbf{r}_j$. Notice that
563 the inner product $\mathbf{r}_{ij} \cdot \mathbf{f}_s^{(ij)}$ is always positive for repulsive feelings.

564

565 The “social pressure function” P_i is roughly similar to the literature defini-
566 tion [10], as expressed in Eq. (4), for neglectable momentum p_i . Furthermore,
567 Eqs. (4) and (A.2) become equal if the area \mathcal{A}_i and r_{ij} are replaced by πr_i^2

568 and the contacting distance $2r_i$, respectively.

569

570 We can further compute the pressure on all the pedestrians according
 571 to Eq. (A.1). Notice that the force sum can be split into the summation
 572 of three contributions: the desire forces, the social forces and the granular
 573 forces. Actually, the granular force does not play a role because of orthog-
 574 onality ($\mathbf{r}_{ij} \cdot \mathbf{f}_g^{(ij)} = 0$). Consequently, replacing Eq. (A.2) into the virial
 575 relation (A.1) gives

576

$$\sum_{i=1}^N \langle 2P_i \mathcal{A}_i \rangle = -2\mathcal{P}\mathcal{A} - \sum_{i=1}^N \langle \mathbf{r}_i \cdot \mathbf{f}_d^{(i)} \rangle \quad (\text{A.3})$$

577 We should remark that Eq. (A.3) holds either if the pedestrians are in
 578 contact or not. The “social pressure function” P_i makes possible for the in-
 579 dividuals to change their behavioural pattern when they come too close to
 580 each other.

581

582 Appendix B. The lane example

583 We decided to open this supplementary section in order to make clear the
 584 meaning of the “social pressure” acting on an individual and the collective
 585 pressure (that is, the *bulk* pressure) on a set of individuals. We will follow a
 586 simple example as a guide for more general situations.

587

588 Appendix B.1. The social pressure

589 Fig. B.13 represents a lane of individuals pushing to the right. The ending
 590 wall prevents the individuals from moving. All the pedestrians in the lane
 591 are at their equilibrium positions $x_1, x_2, \dots, x_i, \dots, x_N$, while the wall is placed
 592 at the position $x_0 = 0$ (see Fig. B.13).

593

594 The pedestrians push to the right acknowledging a desired force $f_d^{(i)} =$
 595 mv_d/τ , according to Eq. (2). The social repulsion feelings balance this desire
 596 force, but only the contacting neighbors are relevant to these feelings. Thus,
 597 the balance equation for any pedestrian in the lane reads

598

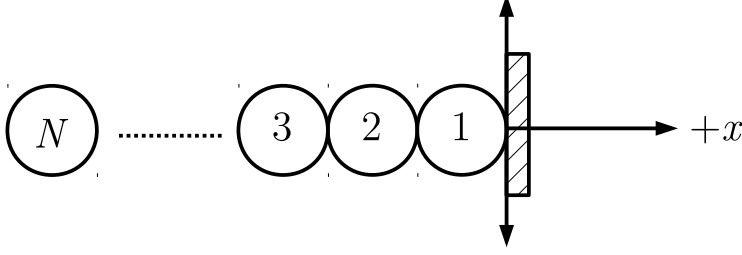


Figure B.13: Lane of individuals pushing to the right. The horizontal axis indicates the positive direction.

$$f_s^{(i,i+1)} - f_s^{(i,i-1)} + \frac{mv_d}{\tau} = 0 \quad (\text{B.1})$$

for $f_s^{(i,j)}$ meaning the repulsive feelings of pedestrian i due to the presence of pedestrian j . Notice that the boundary condition at the wall-end is $x_0 = 0$ (Dirichlet condition), while the condition at the free end is $f_s^{(N,N+1)} = 0$ (Neumann condition). The forces on the pedestrians can be obtained recursively from Eq. B.1, starting at the free ended individual ($i = N$). The resulting expression is

$$f_s^{(i,i-1)} = (N - i + 1) \frac{mv_d}{\tau} \quad , \quad i = 1, \dots, N \quad (\text{B.2})$$

while the corresponding positions $x_1, x_2, \dots, x_i, \dots, x_N$ are obtained by a backward substitution of the social forces expressed in Eq. (2), starting at the wall-end

$$x_i = x_{i-1} - (r_i + r_{i-1}) + B \ln \left[(N - i + 1) \frac{mv_d}{A\tau} \right] \quad (\text{B.3})$$

The pressure on a single pedestrian P_i corresponds to the forces acting on him (her) (per unit length) due to the neighboring pedestrians. According to Eqs. (4), the pressure for any individual i in the lane is

$$P_i = \frac{1}{2\pi r_i} \left[f_s^{(i,i+1)} + f_s^{(i,i-1)} \right] \quad (\text{B.4})$$

We can also arrive to this expression through the “social pressure function” definition (A.2)

$$P_i = \frac{1}{2} \left[\frac{x_i - x_{i+1}}{2\mathcal{A}_i} f_s^{(i,i+1)} + \frac{x_{i-1} - x_i}{2\mathcal{A}_i} f_s^{(i,i-1)} \right] \quad (\text{B.5})$$

613 where the magnitude $x_{ij}/2\mathcal{A}_i$ corresponds to the (inverse) effective length of
 614 the pedestrian. For individuals modeled as circles, the inter-pedestrian dis-
 615 tance is roughly $x_{ij} = 2r_i$ and the area is $\mathcal{A}_i = \pi r_i^2$. Thus, both definitions
 616 agree. However, the last one is preferred since it does not assume that the
 617 forces actuate exactly at the distance r_i , as already mentioned in Section 2.3.
 618

619 *Appendix B.2. The bulk pressure*

620 We can now illustrate on how to compute the virial relation (A.3). We
 621 can add the social pressures expressed in (B.5) for the N pedestrians in the
 622 lane.

$$\left\{ \begin{array}{lcl} 2P_1\mathcal{A}_1 & = & \frac{x_1}{2}f_s^{(1,2)} - \frac{x_2}{2}f_s^{(1,2)} \\ 2P_2\mathcal{A}_2 & = & \frac{x_2}{2}[f_s^{(2,3)} - f_s^{(2,1)}] - \frac{x_3}{2}f_s^{(2,3)} + \frac{x_1}{2}f_s^{(2,1)} \\ 2P_3\mathcal{A}_3 & = & \frac{x_3}{2}[f_s^{(3,4)} - f_s^{(3,2)}] - \frac{x_4}{2}f_s^{(3,4)} + \frac{x_2}{2}f_s^{(3,2)} \\ \dots & & \\ 2P_N\mathcal{A}_N & = & -\frac{x_N}{2}f_s^{(N,N-1)} + \frac{x_{N-1}}{2}f_s^{(N,N-1)} \end{array} \right. \quad (\text{B.6})$$

623 These are the local pressures on each pedestrian due to the contacting
 624 neighbors (and excluding the wall). Adding the terms results in the virial
 625 relation, as expressed in (A.3)

$$\begin{aligned} \sum_{i=1}^N 2P_i\mathcal{A}_i &= (x_1 - x_2)f_s^{(1,2)} + (x_2 - x_3)f_s^{(2,3)} + \dots \\ &+ (x_{N-1} - x_N)f_s^{(N,N-1)} \end{aligned} \quad (\text{B.7})$$

$$= x_1 \frac{N m v_d}{\tau} - \sum_{i=1}^N x_i \frac{m v_d}{\tau}$$

626 where the first term on the right corresponds to the global pressure $-2\mathcal{PA}$.
 627 Notice that x_1 is negative, and thus, $2\mathcal{PA}$ is defined as a positive magnitude.
 628 The last term is also positive, adding pressure to the bulk due to the desire

629 forces.

630

631 The virial relation (A.3) allows to compute the *bulk* pressure on a group
 632 of pedestrians. For example, the pressure on the M pedestrians closest to the
 633 wall corresponds to the force acting on this group due to the other $N - M$
 634 pedestrians. According to Eq. (A.3), the pressure on the M individuals is

$$\sum_{i=1}^M 2P_i \mathcal{A}_i = -2\mathcal{P}\mathcal{A} - \sum_{i=M+1}^N 2P_i \mathcal{A}_i - \sum_{i=1}^N x_i \frac{mv_d}{\tau} \quad (\text{B.8})$$

635 The *bulk* pressure on the first M individuals increases as more individuals
 636 are included in the crowd. This can be verified by evaluating Eq. (B.7) and
 637 Eq. (B.8) for increasing values of N .

638

639 The Eqs. (B.2) and (B.3) allow to compute the pedestrian pressure profile
 640 as a function of the distance to the wall. The profile is qualitatively similar
 641 to the one measured during an evacuation process. Fig. B.14 represents the
 642 histogram for the pressure on each pedestrian, computed as in Eq. 4 and
 643 Eq. A.2 (see caption for details).

644

- 645 [1] W. Cheng, S. Lo, Z. Fang, C. Cheng, A view on the means of fire
 646 prevention of ancient chinese buildings-from religious belief to practice,
 647 Structural Survey 22 (2004) 201209.
- 648 [2] OSHA, Design and construction requirements for exit routes, Occupa-
 649 tional Safety & Health Administration Standards 29-CFR 1910.36(b)
 650 (2015) 1–3.
- 651 [3] FBC2010, Exit and exit access doorways, Florida Building Code Hand-
 652 book 1015.1 (2010) 90.
- 653 [4] FBC2010, Doors, gates and turnstiles, Florida Building Code Handbook
 654 1008.1 (2010) 81.
- 655 [5] A. Kirchner, A. Schadschneider, Simulating of evacuation processes us-
 656 ing a bionics-inspired cellular automaton model for pedestrian dynamics,
 657 Physica A 312 (2002) 260–276.

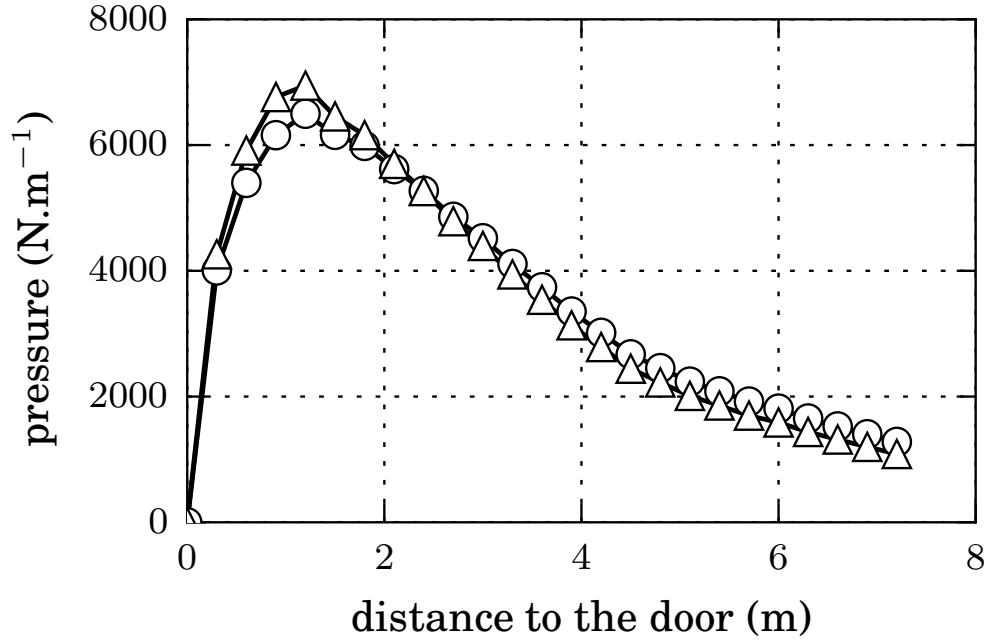


Figure B.14: Mean pressure as a function of the distance to the exit. The room was $20\text{ m} \times 20\text{ m}$ size and included one door of $d_w = 1.2\text{ m}$ width. Mean values were computed from 30 evacuation processes, until 100 pedestrians left the room. The desired velocity was $v_d = 4\text{ m/s}$. The distance to the door was binned into equal intervals of 0.3 m . The \circ symbols correspond to the mean pressure computed as in A.2 for neglectable momentum ($p_i = 0$) and $\mathcal{A}_i = \pi r_i^2$. The symbols \triangle correspond to the mean pressure computed as in 4 (see text for details).

- 658 [6] G. Perez, G. Tapang, M. Lim, C. Saloma, Streaming, disruptive inter-
659 ference and power-law behavior in the exit dynamics of confined pedes-
660 trians, *Physica A* 312 (2002) 609–618.
- 661 [7] Z. Daoliang, Y. Lizhong, L. Jian, Exit dynamics of occupant evacuation
662 in an emergency, *Physica A* 363 (2006) 501–511.
- 663 [8] T. Huan-Huan, D. Li-Yun, X. Yu, Influence of the exits' configuration
664 on evacuation process in a room without obstacle, *Physica A* 420 (2015)
665 164–178.
- 666 [9] D. Parisi, C. Dorso, Microscopic dynamics of pedestrian evacuation,
667 *Physica A* 354 (2005) 606–618.
- 668 [10] D. Helbing, I. Farkas, T. Vicsek, Simulating dynamical features of escape
669 panic, *Nature* 407 (2000) 487–490.
- 670 [11] D. Parisi, C. Dorso, Morphological and dynamical aspects of the room
671 evacuation process, *Physica A* 385 (2007) 343–355.
- 672 [12] G. Frank, C. Dorso, Room evacuation in the presence of an obstacle,
673 *Physica A* 390 (2011) 2135–2145.
- 674 [13] G. Frank, C. Dorso, Evacuation under limited visibility, *International*
675 *Journal of Modern Physics C* 26 (2015) 1–18.
- 676 [14] D. Helbing, P. Molnár, Social force model for pedestrian dynamics, *Phys-*
677 *ical Review E* 51 (1995) 4282–4286.
- 678 [15] M. Mysen, S. Berntsen, P. Nafstad, P. G. Schild, Occupancy den-
679 sity and benefits of demand-controlled ventilation in norwegian
680 primary schools, *Energy and Buildings* 37 (12) (2005) 1234 – 1240.
681 doi:<http://dx.doi.org/10.1016/j.enbuild.2005.01.003>.
682 URL <http://www.sciencedirect.com/science/article/pii/S0378777880500040X>
- 683 [16] S. Plimpton, Fast parallel algorithms for short-range molecular dy-
684 namics, *Journal of Computational Physics* 117 (1) (1995) 1 – 19.
685 doi:<http://dx.doi.org/10.1006/jcph.1995.1039>.
686 URL <http://www.sciencedirect.com/science/article/pii/S002199918571039X>

687 [17] T. W. Lion, R. J. Allen, Computing the local pressure in molecular
688 dynamics simulations, Journal of Physics: Condensed Matter 24 (28)
689 (2012) 284133.
690 URL <http://stacks.iop.org/0953-8984/24/i=28/a=284133>